Cell. Mol. Life Sci. 66 (2009) 1603 – 1616
1420-682X/09/091603-14
DOI 10.1007/s00018-009-9076-8

Cellular and Molecular Life Sciences

Research Article

Interaction between PGE_2 and EGF receptor through MAPKs in mouse embryonic stem cell proliferation

S. P. Yun, M. Y. Lee, J. M. Ryu and H. J. Han*

Department of Veterinary Physiology, Biotherapy Human Resources Center (BK21), College of Veterinary Medicine, Chonnam National University, Gwangju 500 – 757 (Korea), Fax: 82-62-530-2809, e-mail: hjhan@chonnam.ac.kr

Received 30 January 2009; received after revision 03 March 2009; accepted 10 March 2009
Online First 27 March 2009

Abstract. Identifying the small molecules that permit precise regulation of embryonic stem (ES) cell proliferation should further support our understanding of the underlying molecular mechanisms of self renewal. In the present study, we showed that PGE_2 increased [^{3}H]-thymidine incorporation in a time and dose dependent manner. In addition, PGE_2 increased the expression of cell cycle regulatory proteins, the percentage of cells in S phase and the total number of cells. PGE_2 obviously increased E-type prostaglandin (EP) receptor 1 mRNA expression level compare to 2, 3, 4 subtypes. EP1 antagonist also blocked PGE_2-induced cell cycle regulatory protein expression and thymidine incorporation. PGE_2 caused phosphorylation of protine kinase C, Src, epidermal growth factor (EGF) receptor, phosphatidylinositol 3-kinase (PI3K)/Akt phosphorylation, and p44/42 mitogen-activated protein kinase (MAPK), which were blocked by each inhibitors. In conclusion, PGE_2-stimulated proliferation is mediated by MAPK via EP1 receptor-dependent PKC and EGF receptor-dependent PI3K/Akt signaling pathways in mouse ES cells.

Keywords. Mouse ES cells, PGE_2, EP1 receptor, PKC, MAPKs, cell proliferation.

Introduction

Over the last few years a number of extracellular factors have been identified that affect ES cell proliferation. To understand the underlying molecular mechanisms of ES cell proliferation, it would be useful to identify the small molecules that permit precise regulation of ES cell proliferation. In this respect, one of the first issues that must be addressed is the necessity to expand ES cells *in vitro* in chemically-defined conditions. In general, prostaglandins play a crucial role in embryo development and implantation [1 – 4]. PGE_2, one of the prostaglandins, plays a crucial role in hematopoietic stem cell growth and development in both embryonic and adult stem cell homeostasis in simple and complex vertebrate systems [5]. There are also reports that PGE_2 protects mouse ES cells from apoptosis [6] and regulates cell proliferation [7]. In addition, endogenous PGE_2 stimulates proliferation of human mesenchymal stem cells [8]. Therefore, it is possible that PGE_2 in the extracellular plasma environment may be involved in ES cell growth. Although many previous reports have examined the function of PGE_2 in the proliferation of various cell types [9 – 14], the effect of PGE_2 on mouse ES cells has not been elucidated.

* Corresponding author.

The biological effects of PGE_2 are mediated through four different G protein-coupled receptor (GPCR) subtypes: EP1, EP2, EP3 and EP4 [15]. The EP1 receptor activates $G\alpha_q$, eliciting enhanced intracellular Ca^{2+} levels by influencing phosphatidylinositol turnover as well as the membrane association and activation of PKC [6, 16]. Also, PGE_2 induces a concentration-dependent increase in the levels of phosphorylated p44/42 mitogen activated protein kinase (MAPK) through a pathway that requires the activities of PKC, IP_3 receptor, and phospholipase C [17]. However, PGE_2 has an alternative pathway in addition to the general pathway via the EP1 receptor. Previous studies have shown that EGF receptor can cross talk with GPCRs via Src [14, 18–20]. In addition, MAPK phosphorylation and CDK expression are mediated by PGE_2-induced activation of EGF receptor and Akt in various cell types [21–24].

In the present study, mouse ES cells were used as a model for cell proliferation. The ES cells were cultured in Dulbecco's modified Eagle's medium (DMEM) supplemented with leukemia inhibitory factor to maintain their undifferentiated state and to support the derivation and expansion of the ES cells [25, 26]. These cells closely resemble their *in vivo* counterparts and thus provide a stable *in vitro* model of embryo growth and development. Thus, we examined the interaction between PGE_2 and EGF receptor in the proliferation and related signaling pathways in mouse embryonic stem cells.

Materials and methods

Materials. Mouse ES cells were obtained from the American Type Culture Collection (ES-E14TG2a; Manassas, VA). Fetal bovine serum (FBS) was purchased from Biowhittaker (Walkersville, MD). Prostaglandin E_2, SC 51322, bisindolylmaleimide I, staurosporine, PP2, AG 1478, LY 294002, and monoclonal anti-β-actin were obtained from Sigma Chemical Company (St. Louis, MO). Akt inhibitor was purchased from Calbiochem (La Jolla, CA). [^{3}H]-Thymidine was obtained from Dupont/NEN (Boston, MA). Phospho-p44/42, p44/42, phospho-Akt^{Thr308}, phospho-Akt^{Ser473}, and total-Akt antibodies were purchased from New England Biolabs (Herts, UK). Anti-CDK2, cyclin E, CDK4, cyclin D1, p21$^{cip1/waf1}$, p27^{kip1}, PKC α, ε, ζ, phospho-EGFR, and phospho-Src antibodies were purchased from Santa Cruz Biotechnology (Delaware, CA). Goat anti-rabbit IgG antibodies were supplied by Jackson Immunoresearch (West Grove, PA). Liquiscint was obtained from National Diagnostics (Parsippany, NY). All other reagents were of the highest purity commercially available and were used as received.

ES cell culture. Mouse ES cells were cultured for five days in Dulbecco's modified Eagle's media (DMEM, Gibco-BRL, Gaithersburg, MD) supplemented with 3.7 g/L sodium bicarbonate, 1 % penicillin and streptomycin, 1.7 mM L-glutamine, 0.1 mM β–mercaptoethanol, 5 μg/ml mouse leukemia inhibitory factor (LIF), and 15 % FBS, without feeder layer. The cells were grown on gelatinized 12-well plates or 60-mm culture dishes in an incubator maintained at 37 °C in an atmosphere containing 5 % CO_2 and air. After two – three days the cells were washed twice with phosphate-buffered saline (PBS) and maintained in serum-free DMEM with all supplements. After a 24 h incubation period, the cells were washed twice with PBS and incubated with fresh serum-free media including all supplements and the designated agents for the indicated period.

Alkaline phosphatase staining. Cells were washed twice with PBS and fixed with 4 % formaldehyde for approximately 15 min at room temperature. After washing the cells with PBS, cells were incubated with alkaline phosphatase substrate solution [200 μg/ml Naphthol AS-MX phosphate, 2 % N, N dimethylformamide, 0.1 M Tris (pH 8.2), and 1 mg/ml Fast Red TR salt] for approximately 10~15 min at room temperature. After washing with PBS, the cells were photographed.

Immunofluorescence staining with SSEA-1. Cells were fixed and treated with mouse anti-SSEA-1 antibody (1:50, Santa Cruz Biotechnology, Delaware, CA) for 1 h at room temperature. Subsequently, the cells were incubated with fluorescein isothiocyanate-conjugated (FITC-conjugated) anti-mouse IgM (1:100) for 1 h at room temperature. Fluorescence images were obtained using a fluorescence microscope (Fluoview 300, Olympus).

[^{3}H]-thymidine incorporation. [^{3}H]-thymidine incorporation experiments were carried out using the methods described by Brett et al. [27]. In this study, the cells were cultured in a single well until they reached 70 % confluence. They were then washed twice with PBS and maintained in serum-free DMEM including all supplements. After 24 h incubation, the cells were washed twice with PBS and incubated with fresh serum-free DMEM containing all supplements and the indicated agents. After the indicated incubation period, 1 μCi of [methyl-^{3}H]-thymidine was added to the cultures. Incubation with [^{3}H]-thymidine continued for 1 h at 37 °C. The cells were washed twice

with PBS, fixed in 10% trichloroacetic acid (TCA) at 23 °C for 30 min, and then washed twice with 5% TCA. The acid-insoluble material was dissolved in 2 N NaOH for 12 h at 23°C. Aliquots were removed to measure the radioactivity using a liquid scintillation counter. All values are reported as the mean ± S.E. of triplicate experiments. The values were converted from absolute counts to a percentage of the control in order to allow comparison between experiments.

Cell number counting. The cells were incubated with PGE_2 for 24 h as described above and washed twice with PBS. The cells were then detached from the culture dishes utilizing a 0.05% trypsin and 0.5 mM EDTA solution, and the detachment was quenched with soybean trypsin inhibitor (0.05 mg/ml). Subsequently, 0.4% (w/v) trypan blue solution (500 µl) was added to the cell suspension and the cells were counted on a hemocytometer under optical microscopy, while keeping a separate count of the blue cells. Cells failing to exclude the dye were considered nonviable; the data are expressed as the percentage of viable cells.

Bromodeoxyuridine and Oct4 double labeling. For double-labeling experiments, ES cells were synchronized in the G0/G1 phase (by serum starvation for 24 h) and subsequently incubated with 10^{-8} M PGE_2 for 24 h. Cells were then given 15 µM BrdU for an additional 1 h. After several washes with PBS, the cells were fixed in acidic alcohol and processed for Oct4 staining prior to BrdU staining as follows: The fixed cells were incubated with rabbit anti-Oct4 (1:100, Santa Cruz Biotechnology) followed by Alexa Fluor 555 anti-rabbit IgG (1:100, Molecular Probes), each for 1 h at room temperature. After probing, cells were incubated in 1 N HCl, neutralized with 0.1 M sodium tetraborate, and incubated with Alexa Fluor 488-conjugated mouse anti-BrdU for 1 h at room temperature. After washing with PBS, the BrdU/Oct-4 stained cells were examined under confocal microscopy (Fluoview 300; Olympus; Hamburg, Germany).

RNA isolation and reverse transcription-polymerase chain reaction. Total RNA was extracted from mouse ES cells using STAT-60, which is a monophasic solution of phenol and guanidine isothiocyanate purchased from Tel-Test, Inc. (Friendswood, TX, http://www.bioresearchonline.com). Reverse transcription was carried out using 3 µg of RNA using a reverse transcription system kit (AccuPower RT PreMix, Bioneer, Daejeon, Korea, http://www.bioneer.com) with the oligo(dT)18 primers. Five µl of the RT products was then amplified using a polymerase chain reaction (PCR) kit (AccuPower PCR PreMix) under the following conditions: denaturation at 94 °C for 5 min and 30 cycles at 94 °C for 45 s, 55 °C for 30 s, and 72 °C for 30 s, followed by 5 min of extension at 72 °C. The primers used were 5'-CGTGAGACTTTG-CAGCCTGA-3' (sense), 5'-GGCGATGTAAGT-GATCTGCTG-3' (antisense) for Oct4 (519 base pair [bp]); 5'-TCTTACATCGCGCTCATCAC-3' (sense), 5'- TCTTGACGAAGCAGTCGTTG-3' (antisense) for FOXD3 (171 bp); 5'-GTGGAAACTT-TTGTCCGAGAC-3' (sense), 5'-TGGAGTGGGA-GGAAGAGGTAAC-3' (antisense) for SOX2 (550 bp); 5'-GTGCCAAGGGTGGTCCAA-3' (sense), 5'-AACCACTGTGCCGGGAACTA-3' (antisense) for EP1 (550 bp) ; 5'-TGCGCTCAGTCCTCTGTTGT-3' (sense), 5'-TGGCACTGGACTGGGTAGAAC-3' (antisense) for EP2 (654bp); 5'-TCAGATGTCG-GTTGAGCAATG-3' (sense), 5'-AGCCAGGC-GAACTGCAATTA-3' (antisense) for EP3 (382bp); 5'-ACGTCCCAGACCCTCCTGTA-3' (sense), 5'-CGAACCTGGAAGCAAATTCC-3' (antisense) for EP4 (435bp) and 5′-AACCGCGAGAAGATGACC-CAGATCATGTTT-3′ (sense), and 5′-AGCAGCCG-TGGCCATCTCTTGCTCGAAGTC-3′ (antisense) for β-actin (350bp), which was used as a control for the quantity of RNA.

Real time-polymerase chain reaction. Total RNA was extracted from cells treated with each of the designated agents using STAT-60, a monophasic solution of phenol and guanidine isothiocyanate (Tel-Test, Inc.; Friendswood, TX). Real-time quantification of RNA targets was performed in a Rotor-Gene 6000 real-time thermal cycling system (Corbett Research; NSW, Australia) using a QuantiTect SYBR Green RT-PCR kit (QIAGEN; Valencia, CA). We used the same primers as those used for the RT-PCR. The reaction mixture (20 µl) contained 200 ng of total RNA, 0.5 µM of each primer, and the amounts of enzymes and fluorescent dyes recommended by the supplier. The Rotor-Gene 6000 cycler was programmed as follows: 30 min at 50 °C for reverse transcription; 15 min at 95 °C for DNA polymerase activation; 15 s at 95 °C for denaturing; and 45 cycles as follows: 15 s at 94 °C, 30 s at 55 °C, and 30 s at 72 °C. Data was collected during the extension step (30 s at 72 °C) and analyzed using the software provided by the manufacturer. Following PCR, melting curve analysis verified the specificity and identity of the PCR products.

Preparation of cytosolic and total membrane fractions. The cytosolic and total membrane fractions were prepared using a slight modification of the method reported by Mackman et al. [28]. The medium was removed and replaced with serum-free DMEM including all the supplements contained in

the LIF for 12 h prior to the experiments. After removing the medium, the cells were washed twice with ice-cold PBS, scraped, harvested by microcentrifugation, and resuspended in buffer A (137 mM NaCl, 8.1 mM Na_2HPO_4, 2.7 mM KCl, 1.5 mM KH_2PO_4, 2.5 mM EDTA, 1 mM dithiothreitol, 0.1 mM phenylmethylsulfonyl fluoride, 10 μg/ml leupeptin, 0.5 mM sodium orthovanadate, pH 7.5). The resuspended cells were then mechanically lysed on ice by trituration with a 21.1-gauge needle. The cell lysates were initially centrifuged at 1000 *g* for 10 min at 4 °C. The supernatants were collected and centrifuged at 100 000 *g* for 1 h at 4 °C to prepare the cytosolic and total particulate fractions. The supernatant (cytosolic fraction) was then precipitated with five volumes of acetone, incubated on ice for 5 min, and centrifuged at 20 000 *g* for 20 min at 4 °C. The resulting pellet was resuspended in buffer A containing 1 % (vol/vol) Triton X-100. The particulate fractions containing the membrane fraction were washed twice and resuspended in buffer A containing 1 % (vol/vol) Triton X-100.

p44/42 MAPK siRNA transfection. Cells were grown to 75 % confluence in each dish and were transfected for 24 h with either a SMARTpool of siRNA specific for p44 and p42 MAPK (100 nmol/L) or a nontargeting siRNA as a negative control (100 nmol/L; Dharmacon, Inc.) using Lipofectamine 2000 (Invitrogen), according to the manufacturer's instructions.

Western blot analysis. Cells were harvested, washed twice with PBS, and lysed with buffer (20 mM Tris [pH 7.5], 1 mM EDTA, 1 mM EGTA, 1 % Triton X-100, 1 mg/ml aprotinin, and 1 mM phenylmethylsulfonylfluoride) for 30 min on ice. The lysates were then cleared by centrifugation (15 000 rpm at 4 °C for 10 min). Protein concentration was determined by the Bradford method [29]. Equal amounts of protein (20 μg) were resolved by electrophoresis on 10 % SDS-PAGE and transferred to polyvinylidene fluoride membrane. After the blots were washed with TBST (10 mM Tris-HCl [pH 7.6], 150 mM NaCl, and 0.05 % Tween-20), the membranes were blocked with 5 % skimmed milk for 1 h and incubated with an appropriate primary antibody at the dilution recommended by the supplier. The membrane was then washed and primary antibodies were detected with horseradish peroxidase-conjugated secondary antibody. The bands were then visualized by enhanced chemiluminescence (Amersham Pharmacia Biotech, Buckinghamshire, UK).

Fluorescence-activated cell sorting (FACS) analysis. The cells were incubated under PGE_2-treated conditions for 24 h. They were then dissociated in trypsin/EDTA, pelleted by centrifugation, and resuspended at approximately 10^6 cells/ml in PBS containing 0.1 % BSA. The cells were then fixed in 70 % ice-cold ethanol, followed by incubation in freshly prepared nuclei staining buffer (250 μg/ml propidium iodide [PI] and 100 μg/ml RNase) for 30 min at 37 °C. Cell cycle histograms were generated after analyzing the PI-stained cells by flow cytometry (Beckman Coulter, Fullerton, CA). At least 10^4 events were recorded for each sample. The samples were analyzed using CXP software (Beckman Coulter).

Statistical analysis. The results are expressed as means ± standard errors (S.E.). All experiments were analyzed by ANOVA, followed in some experiments by a comparison of treatment means with the control using the Bonferroni-Dunn test. Differences were considered statistically significant when $p < 0.05$.

Result

Effect of PGE_2 on cell proliferation. The undifferentiated state of the mouse ES cells used in this experiment was confirmed by examining the expression of undifferentiated stem cell markers, including the alkaline phosphatase activity, carbohydrate epitope stage-specific embryonic antigen-1 (SSEA-1) expression and Oct-4, SOX-2, and FOXD-3 expression. As shown in Figure 1A and B, mouse ES cells in both the presence and the absence of PGE_2 maintained alkaline phosphatase enzyme activity and expressed SSEA-1, which was detected by immunofluorescent staining. In this study, mouse ES cells treated with PGE_2 expressed Oct-4, SOX-2, and FOXD-3 mRNA (Fig. 1C). In addition, we observed Oct-4 and Nanog protein expression (Fig. 1D) equivalent to that in control cells after treating the cells with PGE_2 (10^{-8} M) for 24 h. Therefore, these results suggest that the mouse ES cells maintained the undifferentiated state under the experimental conditions used in this study.

The effect of PGE_2 on cell proliferation was examined by treating mouse ES cells with 10^{-8} M PGE_2 for various time periods (0–24 h) or with various doses (0-10^{-6} M) for 24 h. As shown in Figure 2A, the maximum increase in the level of [^{3}H]-thymidine incorporation was observed after an 8 h incubation with 10^{-8} M PGE_2 (77 % increase compared to the control; $p < 0.05$). PGE_2, at $\geq 10^{-9}$ M, also increased the level of [^{3}H]-thymidine incorporation in a dose-dependent manner over a 24 h incubation period (Fig. 2B). Cell cycle regulatory protein (CDK2, cyclin E, CDK4, and cyclin D1) levels were also significantly

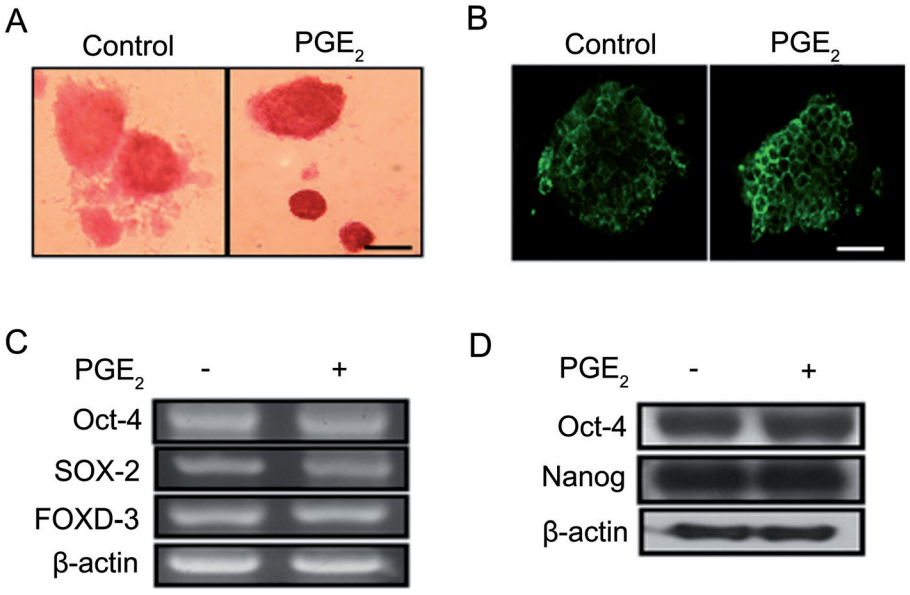

Figure 1. Effect of PGE_2 on mouse ES cell characteristics. (*A*) Alkaline phosphatase (AP) enzyme activity and (*B*) immunofluorescence staining with mouse stage-specific embryonic antigen-1 (SSEA-1) were assessed in mouse ES cells treated in the presence or absence of PGE_2 (10 ng/ml) for 24 h as described in Materials and methods. The scale bars represent 20 μm (magnification ×400). (*C*) Oct-4 (519 bp), SOX-2 (550 bp), FOXD-3 (171 bp), and β-actin (350 bp) mRNA expression levels in the presence or absence of PGE_2. (*D*) Effect of PGE_2 on Oct-4, Nanog, and β-actin protein expression levels. Bands represent 50–60 kDa Oct-4, 35 kDa Nanog, and 41 kDa β-actin, respectively.

increased, but the $p21^{cip1/waf1}$ and $p27^{kip1}$ levels decreased in response to 10^{-8} M PGE_2 (Fig. 2C). To more precisely analyze the effects of PGE_2, we analyzed the cell population by flow cytometry. As shown in Figure 2D, PGE_2 increased the percentage of the cell population in S phase to 33 % as compared to the control. To determine if PGE_2 exerts its growth-promoting effect on undifferentiated ES cells, double labeling for Oct-4 and BrdU expression was performed. In these experiments, the ES cell population contained more than 90 % undifferentiated (Oct-4-positive) cells. The observed effect reflects a role for PGE_2 in proliferation of mouse ES cells, not in spontaneously differentiated progeny (Fig. 2E). Finally, a significant increase in the number of cells was observed in a dose-dependent manner over a 24 h incubation period (Fig. 2F).

Involvement of PGE_2 receptor-dependent PKC activation. In order to examine the role of E-type prostaglandin (EP) receptors and the related pathways in PGE_2-induced cell proliferation, we determined whether PGE_2 induced the expression of EP receptors and cell cycle regulatory proteins in mouse ES cells. As seen in Figure 3A and B, the treatment of PGE_2 (10^{-8} M) increased the mRNA expression of EP1 and EP2 in RT-PCR and real-time PCR analysis. In addition, pretreatment with SC 51322 (10^{-6} M, an EP1 receptor selective antagonist) significantly blocked the PGE_2-induced increase in expression of cell cycle regulatory proteins (Fig. 3C). As shown in Figure 3D and E, SC 51322 reduced the PGE_2-induced increase in $[^3H]$-thymidine incorporation and the percentage of cells in S phase.

In order to examine the role of the PKC pathway in PGE_2-induced cell proliferation via EP1, we assessed whether PGE_2 induced the phosphorylation of pan-PKC in mouse ES cells. As seen in Figure 4A, PGE_2 increased in phosphorylated pan-PKC at 30 min. In addition, PKC α translocated from cytosolic to membrane fraction in response to PGE_2 for 30 min (Fig. 4B). As shown in Figure 4C, SC 51322 reduced the PGE_2-induced phosphorylation of pan-PKC. To further interpret its related signal pathway, we examined the effects of PKC on the PGE_2-induced increase in expression of cell cycle regulatory proteins and $[^3H]$-thymidine incorporation. Mouse ES cells were pretreated with bisindolylmaleimide I and staurosporine (10^{-6} M, PKC inhibitors) prior to PGE_2 treatment. As shown in Figure 4D, E and F, bisindolylmaleimide I and staurosporine reduced the PGE_2-induced increase in expression of cell cycle regulatory proteins, $[^3H]$-thymidine incorporation, and the percentage of cells in S phase.

Involvement of EGF receptor transactivation. Involvement of EGF receptor transactivation in PGE_2-induced increase of cell proliferation was examined. As seen in Figure 5A, EGF receptor phosphorylation increased 5 to 15 min after PGE_2 treatment. In addition, pretreatment with AG 1478 (10^{-6} M, an EGF receptor specific inhibitor) significantly blocked the PGE_2-induced increase in expression of cell cycle regulatory proteins (Fig. 5B), $[^3H]$-thymidine incorporation (Fig. 5C), and percentage of cells in S phase (Fig. 5D). The effect of PGE_2 on the levels of phosphorylation of Src proteins, which are believed to be essential factors in EGF receptor transactiva-

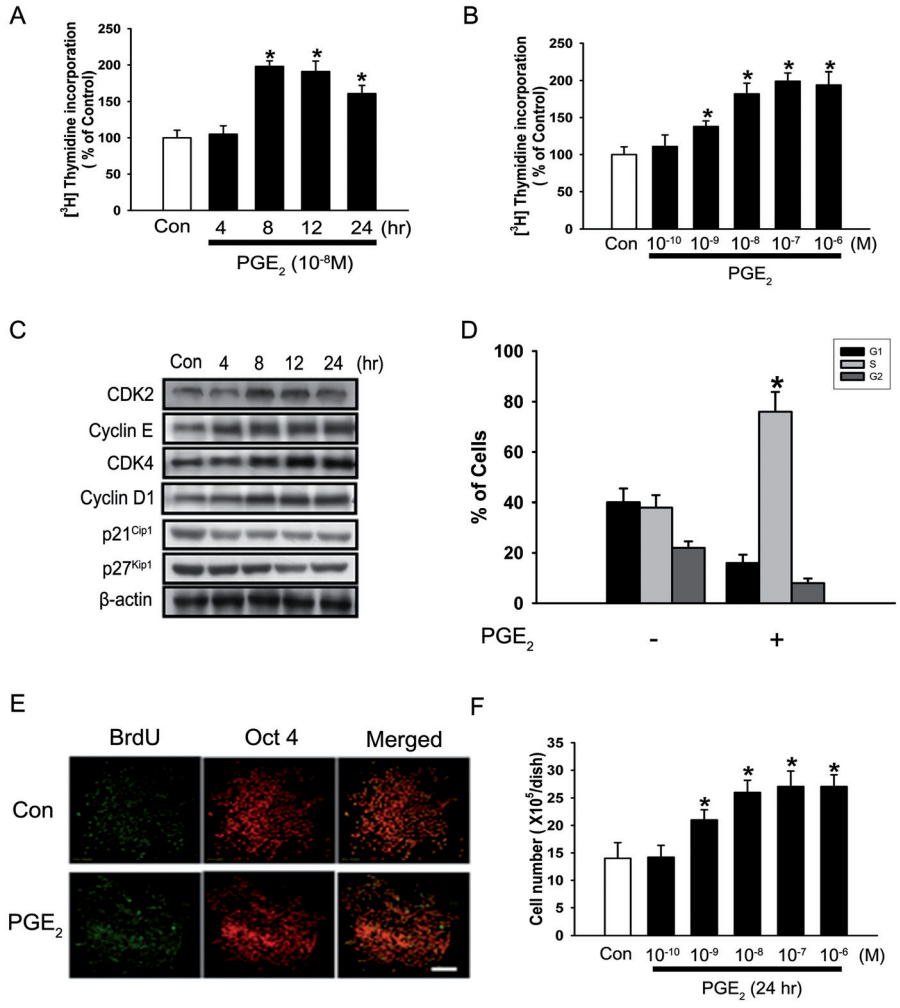

Figure 2. Effects of PGE_2 on mouse ES cell proliferation. Time (*A*) and dose (*B*) response of PGE_2 on [^{3}H]-thymidine incorporation. Mouse ES cells were treated with PGE_2 for various times (0 to 24 h) or with different doses of PGE_2 (0-10^{-6} M) for 24 h and subsequently pulsed with 1 μCi of [^{3}H]-thymidine for 1 h. Values are means ± S.E. of five independent experiments with triplicate dishes. *$P < 0.05$ vs. control. (*C*) Effect of PGE_2 on expression of cell cycle regulatory proteins. Total lysates of mouse ES cells treated with PGE_2 for 24 h were subjected to SDS-PAGE and blotted with CDK2, cyclin E, CDK4, cyclin D1, $p21^{cip1/waf1}$ and $p27^{kip1}$ antibodies. The example shown is a representative of four independent experiments. (*D*) FACS data for the mouse ES cell, which were treated with PGE_2 (10^{-8} M) for 12 h. The cells were washed with PBS, fixed, stained, and analyzed by flow cytometry. The gates were configured manually to determine the percentage of cells in the G1, S, and G2 phases based on the DNA content. The values represent the mean ± S.E. of five independent experiments. *$P < 0.05$ vs. S phase of control. (*E*) Mouse ES cells were incubated with PGE_2 (10^{-8} M) for 24 h and double-labeled with BrdU and Oct-4 antibody. The scale bars represent 20 μm (magnification ×400). (*F*) Mouse ES cells were treated with PGE_2 (0-10^{-10} M) for 2 h, and the number of cells was counted using a hemocytometer. The values represent mean ± S.E. of four independent experiments with triplicate dishes. *$P < 0.05$ vs. control.

tion, was examined in order to confirm the effect of PGE_2 on mouse ES cell proliferation. Phosphorylation of Src increased in response to PGE_2 for 60 min (Fig. 5E) and its effect was inhibited by SC 51322 (Fig. 5F). Also, PP2 (10^{-6} M, a Src inhibitor) reduced PGE_2-induced phosphorylation of EGF receptor (Fig. 5G) and blocked the PGE_2-induced increase in expression of cell cycle regulatory proteins (Fig. 5H), [^{3}H]-thymidine incorporation (Fig. 5I), and percentage of cells in S phase (Fig. 5D).

In order to examine the role of the PI3K/Akt pathway in PGE_2-induced cell proliferation, we determined whether PGE_2 induced the phosphorylation of Akt in mouse ES cells. As seen in Figure 6A, Western blot analysis revealed an increase in phosphorylated-Akt^{thr308} and -Akt^{ser473} at 15 to 30 min after PGE_2 treatment. PGE_2-induced phosphorylation of Akt was attenuated by pretreating the cells with AG 1478 and LY 294002 (10^{-6} M, a PI3K inhibitor) (Fig. 6B). Also, to confirm the involvement of EGF receptor-mediated PI3K/Akt in the PGE_2-induced cell proliferation, we examined the effects of the PI3K/Akt pathway on the PGE_2-induced increase in expression of cell cycle regulatory proteins and [^{3}H]-

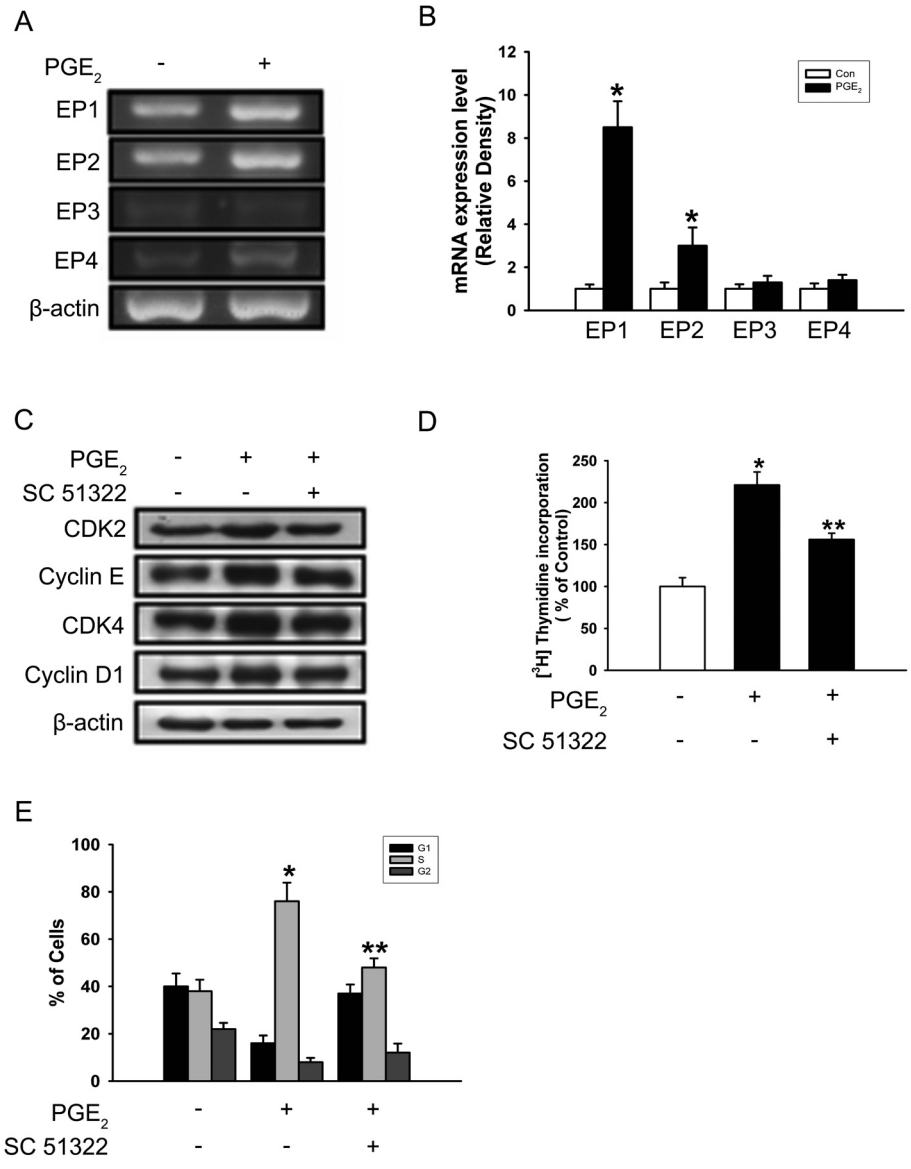

Figure 3. PGE_2 increases proliferation in mouse ES cells via EP receptors expression. Mouse ES cells were incubated with PGE_2 (10^{-8} M) for 12 h. (*A*) Total RNA from mouse ES cells was reverse-transcribed, and EP receptor cDNAs were amplified by polymerase chain reaction as described in Materials and methods. The example shown is a representative of five independent experiments. (*B*) The mRNA expression of EP1, EP2, EP3, and EP4 was measured in mouse ES cells using real-time PCR. The values are reported as the mean ± S.E. of five independent experiments. $*P < 0.05$ vs. control. (*C*) The cells were pretreated with SC 51322 (10^{-6} M , an EP1 receptor-selective antagonist) for 30 min prior to PGE_2 treatment for 12 h. Total protein was extracted and blotted CDK2, cyclin E, CDK4, or cyclin D1, or β-actin antibodies. Each example shown is a representative of four independent experiments. (*D*) The cells were pretreated with SC 51322 for 30 min prior to PGE_2 treatment for 12 h and then with 1 μCi of [^{3}H]-thymidine for 1 h prior to counting. The values represent the mean ± S.E. of five independent experiments with triplicate dishes. $*P < 0.05$ vs. control, $**P < 0.05$ vs. PGE_2 alone. (*E*) FACS data for mouse ES cells that were pretreated with SC 51322 before the 12 h PGE_2 treatment. The cells were washed with PBS, fixed, stained, and analyzed by flow cytometry. The gates were configured manually to determine the percentage of cells in the G1, S, and G2 phases based on DNA content. The values represent the mean ± S.E. of five independent experiments. $*P < 0.05$ vs. S phase of control, $**P < 0.05$ vs. PGE_2 alone.

thymidine incorporation. Mouse ES cells were pretreated with LY 294002 and Akt inhibitor (10^{-5} M) prior to PGE_2 treatment. As shown in Figure 6C, D and E, LY 294002 and Akt inhibitor reduced the PGE_2-induced increase in expression of cell cycle regulatory proteins, [^{3}H]-thymidine incorporation, and percentage of cells in S phase.

Effect of PGE_2 on p44/42 MAPK activation and proliferation. The role of the MAPK pathway in PGE_2-induced cell proliferation was examined by Western blot analysis. As seen in Figure 7A, the phosphorylation of p44/42 MAPK occurred in response to PGE_2. Maximum phosphorylation of p44/42 MAPK appeared 30 min following PGE_2 treatment.

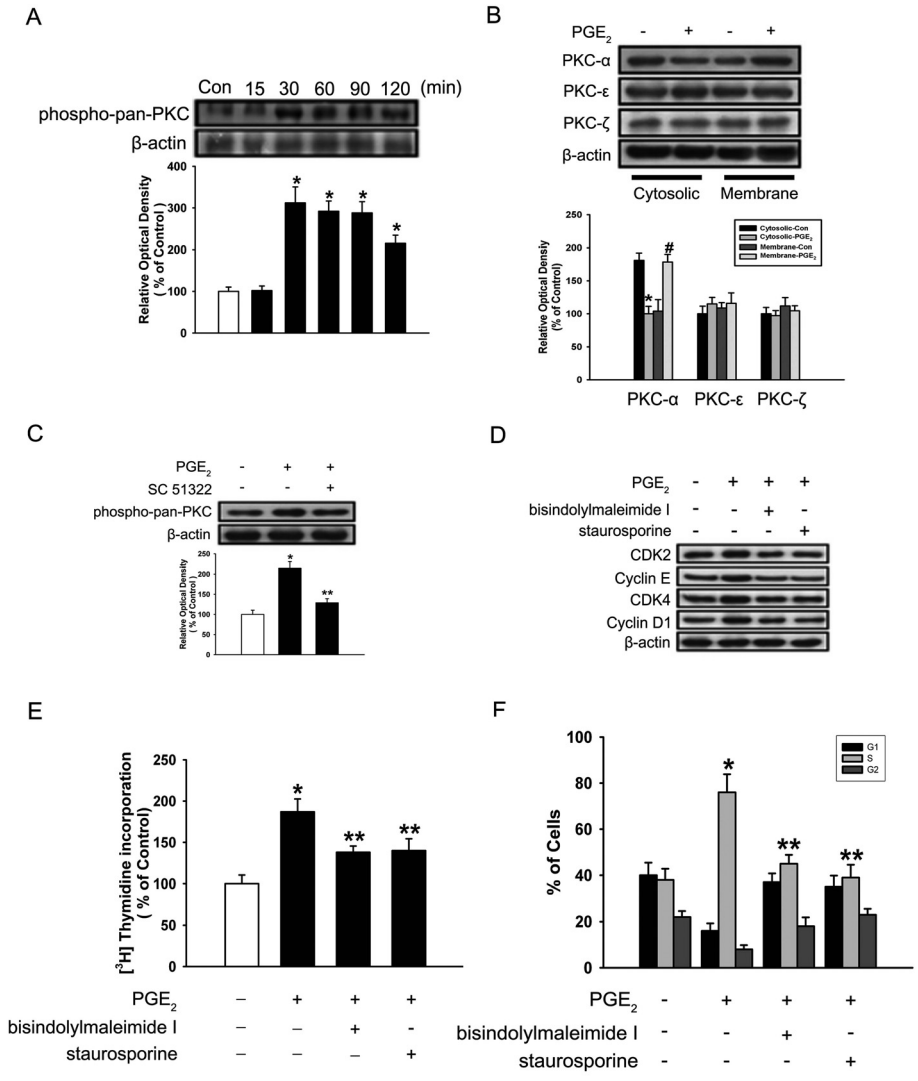

Figure 4. Involvement of PKC pathways in cell proliferation by PGE_2. (*A*) Mouse ES cells were incubated with PGE_2 (10^{-8} M) for 0–120 min and then harvested. Total protein was extracted and blotted with antibody against phospho-pan-PKC. Western blot analysis showed that phosphorylated pan-PKC was increased 30 min after PGE_2 treatment. Each example shown is a representative of five independent experiments. The lower part of (*A*) depicting the bars denotes the mean ± S.E. of five independent experiments for each condition determined from densitometry relative to β-actin. * $P < 0.05$ vs. control. (*B*) Mouse ES cells were stimulated with PGE_2 (10^{-8} M) for 30 min, and then total proteins were extracted for detection of translocation of PKC isoforms. Only PKC α was translocated by PGE_2 treatment. Each example shown is a representative of seven independent experiments. The lower part of (*B*) depicting the bars denotes the mean ± S.E. of seven independent experiments for each condition determined from densitometry relative to β-actin. * $P < 0.05$ vs. cytosolic control, # $P < 0.05$ vs. membrane control. (C) Mouse ES cells were treated with PGE_2 in the presence or absence of SC 51322 (10^{-6} M, an EP1 receptor-selective antagonist), resulting in significant inhibition of PGE_2-induced phospho-pan PKC. Each example shown is a representative of four independent experiments. The lower part of (*C*) depicting the bars denotes the mean ± S.E. of four independent experiments for each condition determined from densitometry relative to β-actin. * $P < 0.05$ vs. control, ** $P < 0.05$ vs. PGE_2 alone. (*D*) The cells were pretreated with bisindolylmaleimide I and staurosporine (10^{-6} M, PKC inhibitors) for 30 min prior to PGE_2 treatment for 12 h. Total protein was extracted and blotted with CDK2, cyclin E, CDK4, cyclin D1, or β-actin antibodies. Each example shown is representative of four independent experiments. (*E*) Cells were pretreated with bisindolylmaleimide I and staurosporine for 30 min prior to PGE_2 treatment for 12 h and then with 1 μCi of [^{3}H]-thymidine for 1 h prior to counting. The values represent the mean ± S.E. of five independent experiments with triplicate dishes. *$P < 0.05$ vs. control, **$P < 0.05$ vs. PGE_2 alone. (*F*) FACS data for mouse ES cells that were pretreated with bisindolylmaleimide I and staurosporine before the 12 h PGE_2 treatment. The cells were washed with PBS, fixed, stained, and analyzed by flow cytometry. The gates were configured manually to determine the percentage of cells in the G1, S, and G2 phases based on DNA content. The values represent the mean ± S.E. of five independent experiments. *$P < 0.05$ vs. S phase of control, **$P < 0.05$ vs. PGE_2 alone.

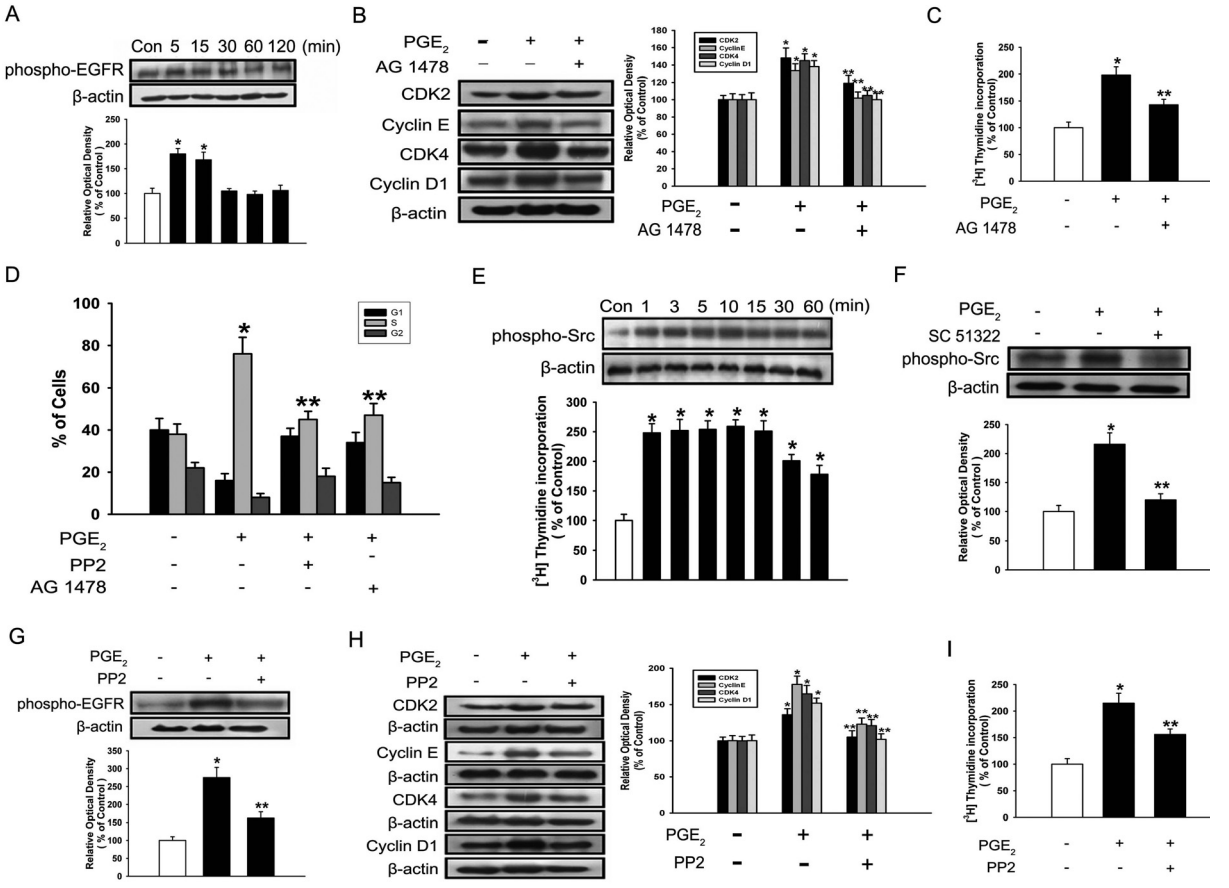

Figure 5. PGE_2-induced proliferation requires transactivation of EGF receptor. (*A*) Mouse ES cells were incubated in the presence of PGE_2 (10^{-8} M) for varying periods of time (0–120 min) and then harvested. Total protein was extracted and blotted with antibody against phosphorylated EGF receptor. Each of the examples shown is a representative of five independent experiments. (*B*) The cells were pretreated with AG 1478 (10^{-6} M, an EGF receptor specific inhibitor) for 30 min prior to PGE_2 treatment for 12 h. Total proteins were extracted and blotted with CDK2, cyclin E, CDK4, cyclin D1, or β-actin antibodies. Each example shown is a representative of seven independent experiments. The right part of (*B*) depicting the bars denotes the mean ± S.E. of seven independent experiments for each condition determined from densitometry relative to β-actin. * $P < 0.05$ vs. control, ** $P < 0.05$ vs. PGE_2 alone. (*C*) The cells were pretreated with AG 1478 for 30 min prior to PGE_2 treatment for 12 h and then with 1 μCi of [^{3}H]-thymidine for 1 h prior to counting. The values represent the mean ± S.E. of five independent experiments with triplicate dishes. *$P < 0.05$ vs. control, **$P < 0.05$ vs. PGE_2 alone. (*D*) FACS data for mouse ES cells that were pretreated with PP2 (10^{-6} M, a Src inhibitor) and AG 1478 before the 12 h PGE_2 treatment. The cells were washed with PBS, fixed, stained, and analyzed by flow cytometry. The gates were configured manually to determine the percentage of cells in the G1, S, and G2 phases based on DNA content. The values represent the mean ± S.E. of four independent experiments. *$P < 0.05$ vs. S phase of control, **$P < 0.05$ vs. PGE_2 alone. (*E*) Mouse ES cells were incubated in the presence of PGE_2 (10^{-8} M) for varying periods of time (0–60 min) and then harvested. Total proteins were extracted and blotted with antibody against Src. Each of the examples shown is representative of five independent experiments. (*F*) Mouse ES cells were treated with PGE_2 in the presence or absence of SC 51322 (10^{-6} M, an EP1 receptor-selective antagonist), resulting in significant inhibition of PGE_2-induced Src phosphorylation. Each example shown is representative of five experiments. (*G*) Mouse ES cells were treated with PGE_2 in the presence or absence of PP2, resulting in significant inhibition of PGE_2-induced EGF receptor phosphorylation. Each example shown is representative of five experiments. The lower part of (A, E, F, and G) depicting the bars denotes the mean ± S.E. of five independent experiments for each condition determined from densitometry relative to β-actin. * $P < 0.05$ vs. control, ** $P < 0.05$ vs. PGE_2 alone. (*H*) The cells were pretreated with PP2 for 30 min prior to PGE_2 treatment for 12 h. Total proteins were extracted and blotted with CDK2, cyclin E, CDK4, or cyclin D1, or β-actin antibodies. Each example shown is representative of seven independent experiments. The right part of (*H*) depicting the bars denotes the mean ± S.E. of seven independent experiments for each condition determined from densitometry relative to β-actin. * $P < 0.05$ vs. control, ** $P < 0.05$ vs. PGE_2 alone. (*I*) The cells were pretreated with PP2 for 30 min prior to PGE_2 treatment for 12 h and then with 1 μCi of [^{3}H]-thymidine for 1 h prior to counting. The values represent the mean ± S.E. of five independent experiments with triplicate dishes. *$P < 0.05$ vs. control, **$P < 0.05$ vs. PGE_2 alone.

Next, we observed the interaction between MAPK and PKC/PI3K. PGE_2-induced phosphorylation of p44/42 MAPK was attenuated by pretreating the cells with bisindolylmaleimide I, staurosporine (PKC inhibitors) (Fig. 7B) and Akt inhibitor (Fig. 7C). To further elucidate the involvement of p44/42 MAPK in the E_2-induced cell proliferation, the mouse ES cells were transfected with a pool of p44 and 42 MAPK specific siRNA (100 nmol/L) or non-targeting siRNA (100 nmol/L) prior to PGE_2 treatment. p44 and p42

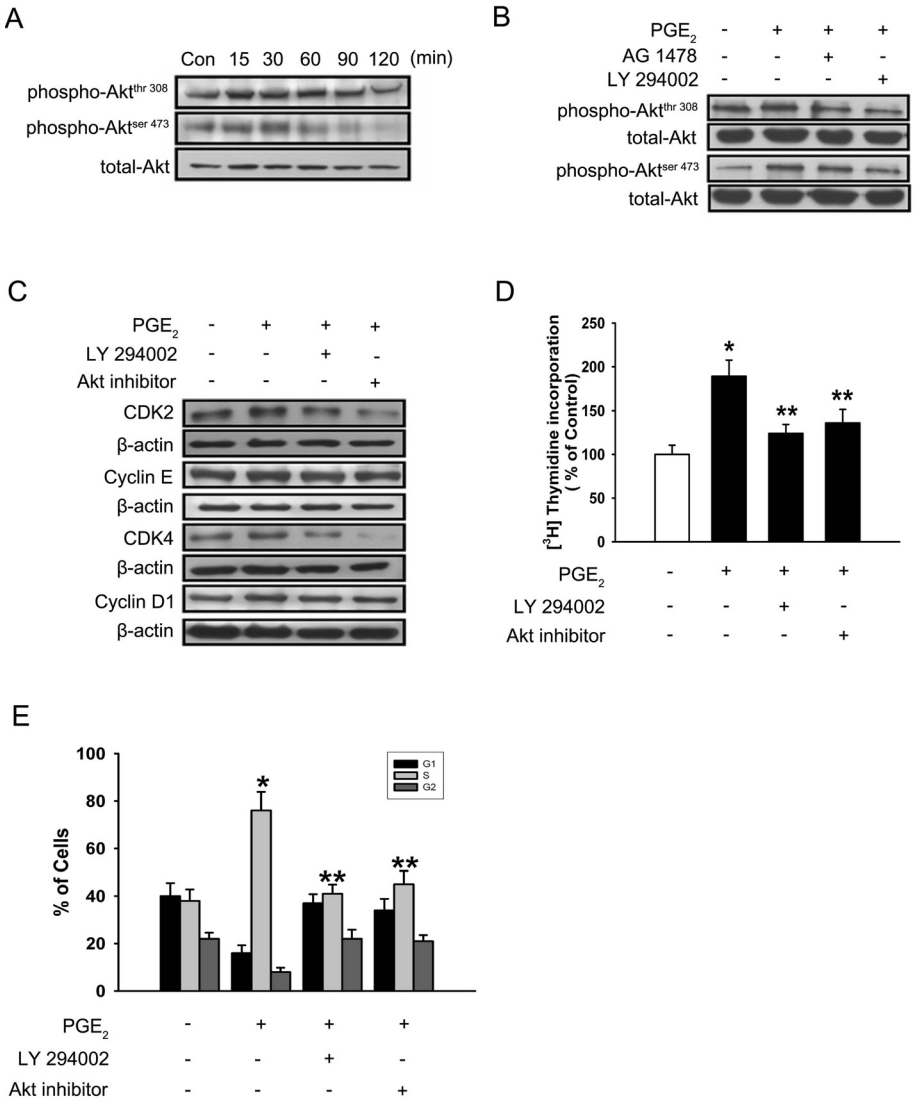

Figure 6. Effect of PGE_2 on Akt activation and cell proliferation. (*A*) Mouse ES cells were treated with PGE_2 (10^{-8} M) for different time periods (0–120 min). The phosphorylation of Akt Thr^{308} and Ser^{473} were detected as described in Materials and methods. Each example shown is a representative of four experiments. (*B*) Mouse ES cells were treated with PGE_2 in the presence or absence of AG 1478 (10^{-6} M, an EGF receptor specific inhibitor) and LY 294002 (10^{-6} M, a PI3K inhibitor), resulting in significant inhibition of PGE_2-induced Akt phosphorylation. Each example shown is representative of four independent experiments. (*C*) The cells were pretreated with LY 294002 or Akt inhibitor (10^{-5} M) for 30 min prior to PGE_2 treatment for 12 h. Total proteins were extracted and blotted with CDK2, cyclin E, CDK4, cyclin D1, or β-actin antibodies. Each example shown is a representative of five independent experiments. (*D*) The cells were pretreated with LY 294002, or Akt inhibitor for 30 min prior to treatment with PGE_2 (10^{-8} M) for 12 h and then with 1 μCi of [^{3}H]-thymidine for 1 h. The values represent the mean ± S.E. of five independent experiments with triplicate dishes. $^*P < 0.05$ vs. control, $^{**}P < 0.05$ vs. PGE_2 alone. (*E*) FACS data for mouse ES cells that were pretreated with LY 294002 and Akt inhibitor before the 12 h PGE_2 treatment. The cells were washed with PBS, fixed, stained, and analyzed by flow cytometry. The gates were configured manually to determine the percentage of cells in the G1, S, and G2 phases based on DNA content. The values represent the mean ± S.E. of five independent experiments. $^*P < 0.05$ vs. S phase of control, $^{**}P < 0.05$ vs. PGE_2 alone.

specific siRNA reduced the PGE_2-induced increase in p44/42 MAPK expression (Fig. 7D). In addition, as shown in Figures 7E, F and G, p44 and 42 MAPK specific siRNA reduced the PGE_2-induced increase in expression of cell cycle regulatory proteins, [^{3}H]-thymidine incorporation, and percentage of cells in S phase.

Discussion

The results of our study demonstrate that PGE_2 stimulates proliferation of mouse ES cells which is mediated by MAPK via EP1 receptor-dependent PKC and EGF receptor-dependent PI3K/Akt signaling pathways in mouse ES cells. The effect of PGE_2 was measured at 10^{-10} M-10^{-6} M concentrations,

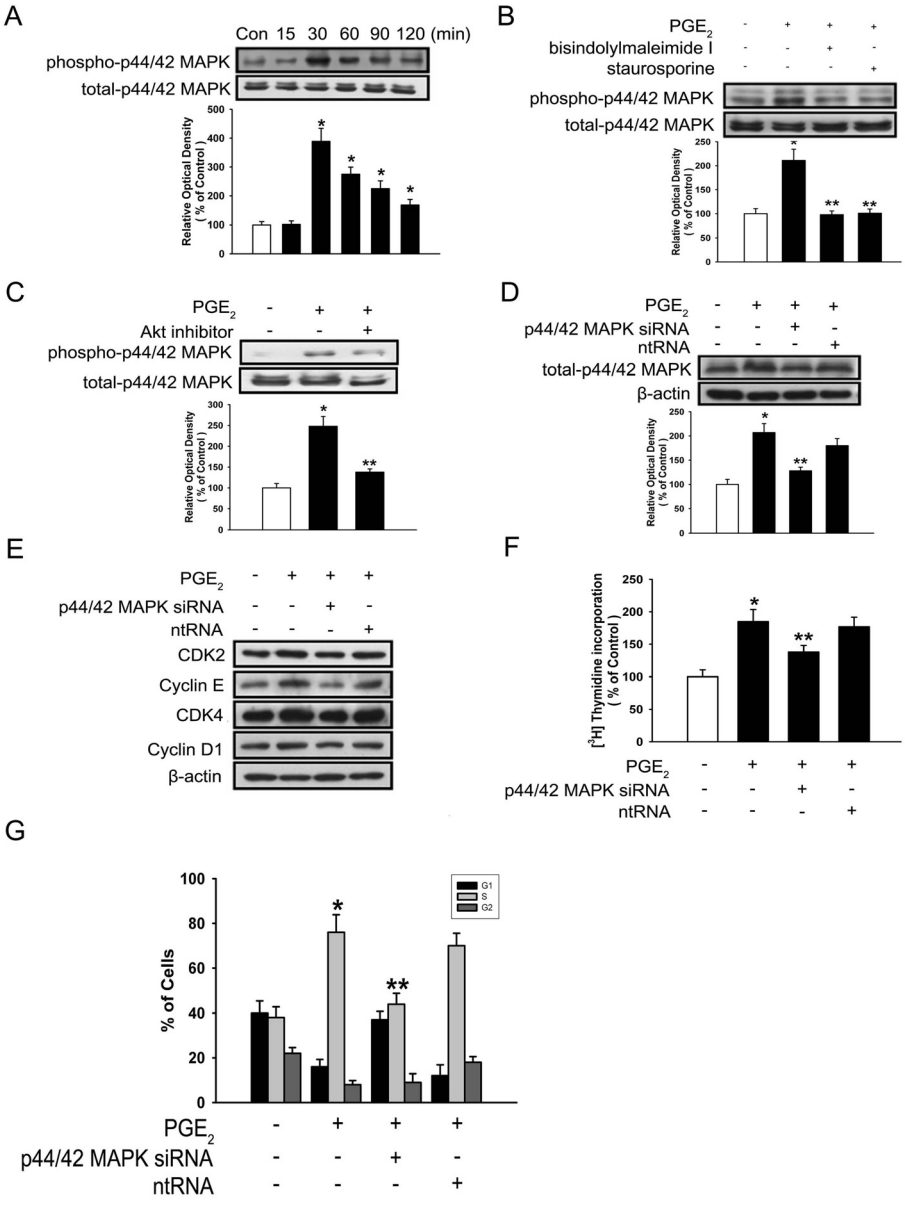

Figure 7. Effect of PGE_2 on p44/42 MAPK activation and cell proliferation. (*A*) Mouse ES cells were treated with PGE_2 (10^{-8} M) for 0–120 min. Total proteins were extracted for detection with phospho-p44/42 MAPK and total-p44/42 MAPK antibodies. Each example shown is representative of five experiments. (*B*) The cells were pretreated with bisindolylmaleimide I and staurosporine (10^{-6} M, PKC inhibitors) for 30 min prior to treatment with PGE_2 for 30 min and the total lysates were subjected to SDS-PAGE and blotted with phospho-p44/42 MAPK and total-p44/42 MAPK antibodies. Each example shown is a representative of five independent experiments. (*C*) The cells were pretreated with Akt inhibitor (10^{-5} M) for 30 min prior to treatment with PGE_2 for 30 min and the total lysates were subjected to SDS-PAGE and blotted with phospho-p44/42 MAPK and total-p44/42 MAPK antibodies. Each example shown is a representative of five independent experiments. (*D*) The mouse ES cells were transfected for 48 h with either a SMARTpool of p44 and p42 MAPKs siRNA (200 pmol/L) or a non-targeting control siRNA (200 pmol/L) using LipofectAMINE 2000 before the 1 h PGE_2 treatment, and then p44/42 MAPK expression was analyzed using Western blot. Each of the examples shown is representative of five independent experiments. The lower part of (*A*, *B*, *C*, and *D*) depicting the bars denotes the mean ± S.E. of five independent experiments for each condition determined from densitometry relative to total-p44/42 MPAK. * $P < 0.05$ vs. control, ** $P < 0.05$ vs. PGE_2 alone. (*E*) The mouse ES cells were transfected for 48 h with either a SMARTpool of p44 and p42 MAPKs siRNA (200 pmol/L) or a non-targeting control siRNA (200 pmol/L) using LipofectAMINE 2000 before the 1 h PGE_2 treatment, and then total protein was extracted and blotted with CDK2, cyclin E, CDK4, cyclin D1, or β-actin antibodies. Each example shown is a representative of four independent experiments. (*F*) Mouse ES cells were transfected for 48 h with either a SMARTpool of p44 and p42 MAPKs siRNA (200 pmol/L) or a non-targeting control siRNA (200 pmol/L) using LipofectAMINE 2000 before the 1 h PGE_2 treatment for 12 h, and then with 1μCi of [^{3}H] thymidine for 1 h prior to counting. The values represent the mean ± S.E. of five independent experiments with triplicate dishes. *$P < 0.05$ vs. control, **$P < 0.05$ vs. PGE_2 alone. (*G*) FACS data for the mouse ES cells, which were pretreated with p44 and p42 MAPKs siRNA before the 12 h E_2 treatment. The cells were washed with PBS, fixed, stained, and analyzed by flow cytometry. The gates were configured manually to determine the percentage of cells in the G1, S, and G2 phases based on the DNA content. The values represent the mean ± S.E. of five independent experiments. *$P < 0.05$ vs. S phase of control, **$P < 0.05$ vs. PGE_2 alone.

representing physiological conditions, although the normal serum concentration of PGE_2 depends on the species to some extent [30]. Our findings strongly suggest that PGE_2 plays a pivotal role in stimulating cell proliferation. In general, the primary action of PGE_2 is mediated by the EP receptors: EP1, EP2, EP3 and EP4 [14, 31–35]. EP1 receptors activate phospholipase C and phosphatidylinositol turnover and stimulate the release of intracellular calcium [36]. Moreover, PGE_2 has recently been reported to enhance the MAPKs pathway through EP1 receptor, calcium, and EGF receptor signaling in human cholangiocarcinoma cells [14]. Therefore, we first examined the correlation between the effect of PGE_2 and EP receptors. Among the EP receptors examined, EP1 receptor had the highest mRNA expression level. This suggests a major potential role for this receptor in the regulation of mouse ES cell proliferation in conjunction with PGE_2 although there is the possibility that the EP2 receptor is also involved in a proliferative effect of PGE_2, since EP2 mRNA level is up-regulated and that the EP1 antagonist did not completely bring proliferation back down to control level. Furthermore, SC 51322 (an EP1 selective antagonist) decreased the expression of cell cycle regulatory proteins, as well as [^{3}H]-thymidine incorporation, and the percentage of cells in the S phase. Therefore, our data strongly suggest that EP1 plays an important role in the effect of PGE_2 in mouse ES cells. Various reports have suggested that PGE_2 interacts with cell surface binding sites (EP1) and induces phosphorylation of PKC [37, 38]. The present study suggests that PGE_2 is linked to the activation of the EP1-mediated PKC pathway in mouse ES cells. For that reason, we hypothesized that EP1 is linked to the phosphorylation of PKC and proliferation in mouse ES cells. We observed that PKC translocates from the cytosol to the membrane fraction. We identified that only PKC α was activated in response to PGE_2. We also observed the effect of SC 51322 on PGE_2-induced phosphorylation of PKC. Furthermore, bisindolymaleimide I and staurosporine (PKC inhibitors) decreased the expression of cell cycle regulatory proteins, as well as the [^{3}H]-thymidine incorporation and the percentage of cells in the S phase. These results suggest that PKC activation plays an important role in PGE_2-induced mouse ES cell proliferation.

In our previous study, we reported that EGF leads to increased protein levels of CDKs and [^{3}H]-thymidine incorporation in proliferating mouse ES cells [37, 39]. Generally, GPCRs can transactivate EGF receptor through several mechanisms, including extracellular release of EGF and other EGF-like ligands or through intracellular molecules including Src-family tyrosine kinases and the inhibitory effects of reactive oxygen species on EGF receptor-specific phosphatases [23, 40, 41]. The present data show that treating mouse ES cells with PGE_2 leads to phosphorylation of Src and EGF receptor in a time-dependent manner. Furthermore, the phosphorylation of Src and EGF receptor was decreased by SC 51322 and PP2 in mouse ES cells. Likewise, our results indicate that the expression levels of CDK 2, cyclin E, CDK 4, and cyclin D1 as well as the [^{3}H]-thymidine incorporation and the percentage of cells in S phase are decreased by the inhibition of these pathways with PP2 and AG 1478. This finding suggests that the EP1-mediated EGF receptor transactivation signaling pathway is involved in the mechanisms of PGE_2-induced cell proliferation in mouse ES cells and offers new hints for alternative strategies to regulate proliferation, such as the use of compounds targeting the EGF receptor signaling cascade.

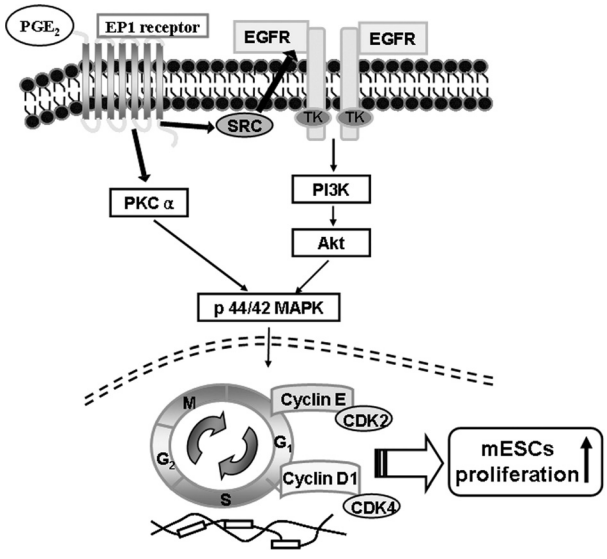

Figure 8. The hypothetical model for the proposed signaling network involved in PGE_2-induced ES cells proliferation. PGE_2 activates EP1 receptor, which increases PKC activity as well as phosphorylation of EGFR via Src. EP1 receptor-dependent PKC and EGF receptor-dependent PI3K/Akt signaling pathways stimulated p44/42 MAPK activity, which increased cyclin E/CDK2 and cyclin D1/CDK4 protein expression levels. PGE_2, Prostaglandin E_2; EP1, E-type prostaglandin receptor 1; EGFR, epidermal growth factor receptor; PI3K, phosphatidylinositol 3-kinase; p44/42 MAPK, p44/42 mitogen-activated protein kinase; CDK, cyclin-dependent kinase.

In general, p44/42 MAPK is involved in various cellular processes, including mitogenic signaling [42–44]. Previous studies have demonstrated that the PGE_2-induced phosphorylation of p44/42 MAPK in human cholangiocarcinoma cells is mediated by EP1 [14]. Phosphorylation of PKC and Akt by this mechanism results in phosphorylation of p44/42 MAPK and stimulation of downstream anti-apoptotic

signaling [31, 45]. Thus, we hypothesized that PKC and PI3K/Akt are linked to activation of the MAPK pathway and proliferation in mouse ES cells. In the present study, the activation of p44/42 MAPK by PGE_2 was blocked by PKC inhibitors, indicating that PGE_2 regulated p44/42 MAPK activity through the PKC pathway. The present data show that treating mouse ES cells with PGE_2 led to phosphorylation of Akt at the Thr^{308} and Ser^{473} sites and of p44/42 MAPK in a time-dependent manner. The activation of Akt by PGE_2 was blocked by AG 1478 (an EGF receptor specific inhibitor), and LY 294002 and Akt inhibitor prevented PGE_2-induced p44/42MAPK phosphorylation. In addition, PGE_2-induced phosphorylation of p44/42 MAPK led to activation of CDKs in human prostate cancer cell lines [24]. Furthermore, in human thyroid tumor cells, p44/42 MAPK inhibitor prevented EGF-induced stimulation of cyclin D1, which is an important intermediate in inducing the cell cycle cascade [46]. In the present study, we demonstrated that PGE_2-induced stimulation of cell cycle regulatory proteins, [^{3}H]-thymidine incorporation, and the percentage of cells in the S phase was blocked by LY 294002, Akt inhibitor and p44/42 MAPK-specific siRNA transfection. These results suggest that the activation of p44/42 MAPK plays a critical role in PGE_2-induced proliferation of mouse ES cells (Fig. 8). The discovery of the role played by PGE_2 in stimulating ES cells proliferation, together with the other results shown in this study, represent a significant advance in our knowledge of how ES cell pluripotency is maintained by PGE_2 and can be applied to the development of increasingly chemically defined ES cell culture systems. In conclusion, PGE_2-stimulated proliferation is mediated by MAPK via EP1 receptor-dependent PKC and EGF receptor-dependent PI3K/Akt signaling pathways in mouse ES cells.

Acknowledgements. This study was supported by a grant (SC2270) from the Stem Cell Research Center of 21st Century Frontier Research Program and graduate fellowship through the Brain Korea 21 project provided by the Ministry of Education, Science and Technology, Republic of Korea.

1 Huang, J. C., Goldsby, J. S., Arbab, F., Melhem, Z., Aleksic, N. and Wu, K. K. (2004) Oviduct prostacyclin functions as a paracrine factor to augment the development of embryos. Hum. Reprod. 19, 2907–2912.
2 Huang, J. C., Wun, W. S., Goldsby, J. S., Wun, I. C., Noorhasan, D. and Wu, K. K. (2007) Stimulation of embryo hatching and implantation by prostacyclin and peroxisome proliferator-activated receptor δ activation: implication in IVF. Hum. Reprod. 22(3), 807–814.
3 Lim, H., Gupta, R. A., Ma, W. G., Paria, B. C., Moller, D. E., Morrow, J. D., DuBois, R. N., Trzaskos, J. M. and Dey, S. K. (1999) Cyclo-oxygenase-2-derived prostacyclin mediates embryo implantation in the mouse via PPARδ. Genes. 13, 1561–1574.
4 Liu, C. H., Lee, M. S., Hsieh, C. H., Huang, C. C., Tsao, H. M. and Hsieh, Y. S. (2006) Prostacyclin enhances mouse embryo development and hatching but not increased embryonic cell number and volume. Fertil. Steril. 86, 1047–1052.
5 North, T. E., Goessling, W., Walkley, C. R., Lengerke, C., Kopani, K. R., Lord, A. M., Weber, G. J., Bowman, T. V., Jang, I. H., Grosser, T., Fitzgerald, G. A., Daley, G. Q., Orkin, S. H. and Zon, L. I. (2007) Prostaglandin E_2 regulates vertebrate haematopoietic stem cell homeostasis. Nature. 447, 1007–1011.
6 Liou, J. Y., Ellent, D. P., Lee, S., Goldsby, J., Ko, B. S., Matijevic, N., Huang, J. C. and Wu, K. K. (2007) Cyclooxygenase-2-derived prostaglandin E_2 protects mouse embryonic stem cells from apoptosis. Stem Cells. 25(5), 1096–1103.
7 Kim, Y. H. and Han, H. J. (2008) High-glucose-induced prostaglandin E_2 and peroxisome proliferator-activated receptor δ promote mouse embryonic stem cell proliferation. Stem Cells. 26(3), 745–755.
8 Arikawa, T., Omura, K. and Morita, I. (2004) Regulation of bone morphogenetic protein-2 expression by endogenous prostaglandin E_2 in human mesenchymal stem cells. J. Cell. Physiol. 200, 400–406.
9 Cherukuri, D. P., Chen, X. B., Goulet, A. C., Young, R. N., Han, Y., Heimark, R. L., Regan, J. W., Meuillet, E. and Nelson, M. A. (2007) The EP4 receptor antagonist, L-161,982, blocks prostaglandin E_2-induced signal transduction and cell proliferation in HCA-7 colon cancer cells. Exp. Cell. Res. 313, 2969–2979
10 Krause, P., Singer, E., Darley, P. I., Klebensberger, J., Groettrup, M. and Legler, D. F. (2007) Prostaglandin E_2 is a key factor for monocyte-derived dendritic cell maturation: enhanced T cell stimulatory capacity despite IDO. J. Leukoc. Biol. 82(5), 1106–1114.
11 Lim, K., Han, C., Xu, L., Isse, K., Demetris, A. J. and Wu, T. (2008) Cyclooxygenase-2-derived prostaglandin E_2 activates β-catenin in human cholangiocarcinoma cells: evidence for inhibition of these signaling pathways by ω 3 polyunsaturated fatty acids. Cancer Res. 68(2), 553–560.
12 Mendez, M. and LaPointe, M. C. (2005) PGE_2-induced hypertrophy of cardiac myocytes involves EP4 receptor-dependent activation of p42/44 MAPK and EGFR transactivation. Am. J. Physiol. Heart Circ. Physiol. 288(5), 2111–2117.
13 Rao, R., Redha, R., Macias-Perez, I., Su, Y., Hao, C., Zent, R., Breyer, M. D. and Pozzi, A. (2007) Prostaglandin E_2-EP4 receptor promotes endothelial cell migration via ERK activation and angiogenesis in vivo. J. Biol. Chem. 282(23), 16959–16968.
14 Zhang, L., Jiang, L., Sun, Q., Peng, T., Lou, K., Liu, N. and Leng, J. (2007) Prostaglandin E_2 enhances mitogen-activated protein kinase/Erk pathway in human cholangiocarcinoma cells: involvement of EP1 receptor, calcium and EGF receptors signaling. Mol. Cell. Biochem. 305(1–2), 19–26.
15 Williams, J. A., Pontzer, C. H. and Shacter, E. (2000) Regulation of macrophage interleukin-6 (IL-6) and IL-10 expression by prostaglandin E_2: The role of p38 mitogen-activated protein kinase. J. Interferon Cytokine Res. 2000. 20, 291–298.
16 Tang, C. H., Yang, R. S. and Fu, W. M. (2005) Prostaglandin E_2 stimulates fibronectin expression through EP1 receptor, phospholipase C, protein kinase Cα, and c-Src pathway in primary cultured rat osteoblasts. J. Biol. Chem. 280(24), 22907–22916.
17 Nirodi, C. S., Crews, B. C., Kozak, K. R., Morrow, J. D. and Marnett, L. J. (2004) The glyceryl ester of prostaglandin E_2 mobilizes calcium and activates signal transduction in RAW264.7 cells. Proc. Natl. Acad. Sci. U S A. 101(7), 1840–1845.
18 Han, C., Demetris, A. J., Stolz, D. B., Xu, L., Lim, K. and Wu, T. (2006) Modulation of Stat3 activation by the cytosolic phospholipase A_2α and cyclooxygenase-2-controlled prostaglandin E_2 signaling pathway. J. Biol. Chem. 281(34):24831–24846.
19 Hart, S., Fischer, O. M., Prenz, I. N., Zwick-Wallasch, E., Schneider, M., Hennighausen, L. and Ullrich, A. (2005)

GPCR-induced migration of breast carcinoma cells depends on both EGFR signal transactivation and EGFR-independent pathways. Biol. Chem. 386, 845–855.
20 Pai, R., Soreghan, B., Szabo, I. L., Pavelka, M., Baatar, D. and Tarnawski, A. S. (2002) Prostaglandin E_2 transactivates EGF receptor: a novel mechanism for promoting colon cancer growth and gastrointestinal hypertrophy. Nature Med. 8, 289–293.
21 Daub, H., Weiss, F. U., Wallasch, C. and Ullrich, A. (1996) Role of transactivation of the EGF receptor in signalling by G-protein-coupled receptors. Nature. 379, 557–560.
22 Pierce, K. L., Tohgo, A., Ahn, S., Field, M. E., Luttrell, L. M. and Lefkowitz, R. J. (2001) Epidermal growth factor (EGF) receptor-dependent ERK activation by G protein-coupled receptors: a co-culture system for identifying intermediates upstream and downstream of heparin-binding EGF shedding. J. Biol. Chem. 276, 23155–23160.
23 Wetzker, R. and Bohmer, F. D. (2003) Transactivation joins multiple tracks to the ERK/MAPK cascade. Nat. Rev. Mol. Cell Biol. 4, 651–657.
24 Ye, F., Jiang, S., Volshonok, H., Wu, J. and Zhang, D. Y. (2007) Molecular mechanism of anti-prostate cancer activity of Scutellaria baicalensis extract. Nutr. Cancer. 57(1), 100–110.
25 Evans, M. J. and Kaufman, M. H. (1981) Establishment in culture of pluripotential cells from mouse embryos. Nature. 292, 154–156.
26 Xie, X., Chan, R. J. and Yoder, M. C. (2002) Thrombopoietin acts synergistically with LIF to maintain an undifferentiated state of embryonic stem cells homozygous for a Shp-2 deletion mutation. FEBS Lett. 529, 361–364.
27 Brett, C. M., Washington, C. B., Ott, R. J., Gutierrez, M. M. and Giacomini, K. M. (1993) Interaction of nucleoside analogues with the sodium-nucleoside transport system in brush border membrane vesicles from human kidney. Pharm. Res. 10, 423–426.
28 Mackman, N., Brand, K. and Edgington, T. S. (1991) Lipopolysaccharide-mediated transcriptional activation of the human tissue factor gene in THP-1 monocytic cells requires both activator protein 1 and nuclear factor κB binding sites. J. Exp. Med. 174, 1517–1526.
29 Bradford, M. M. (1976) A rapid and sensitive method for the quantization of microgram quantities of protein utilizing the principle of protein-dye binding. Anal. Biochem. 72, 248–254.
30 Sylvia, V. L., Del Toro, F. Jr., Hardin, R. R., Dean, D. D., Boyan, B. D. and Schwartz, Z. (2001) Characterization of PGE_2 receptors (EP) and their role as mediators of $1\alpha,25\text{-}(OH)_2D_3$ effects on growth zone chondrocytes. J. Steroid Biochem. Mol. Biol. 78(3), 261–274.
31 Dajani, O. F., Meisdalen, K., Guren, T. K., Aasrum, M., Tveteraas, I. H., Lilleby, P., Thoresen, G. H., Sandnes, D. and Christoffersen, T. (2008) Prostaglandin E_2 upregulates EGF-stimulated signaling in mitogenic pathways involving Akt and ERK in hepatocytes. J. Cell. Physiol. 214, 371–380.
32 Minami, T., Nakano, H., Kobayashi, T., Sugimoto, Y., Ushikubi, F., Ichikawa, A., Narumiya, S. and Ito, S. (2001) Characterization of EP receptor subtypes responsible for prostaglandin E_2-induced pain responses by use of EP1 and EP3 receptor knockout mice. Br. J. Pharmacol. 133(3), 438–444.
33 Walch, L., Clavarino, E. and Morris, P. L. (2003) Prostaglandin (PG) FP and EP1 receptors mediate $PGF_2\alpha$ and PGE_2 regulation of interleukin-1β expression in Leydig cell progenitors. Endocrinology. 144(4), 1284–1291.
34 Wise, H. and Jones, R. L. (1994) Characterization of prostanoid receptors on rat neutrophils. Br. J. Pharmacol. 113(2), 581–587.
35 Zhang, Y., Guan, Y., Schneider, A., Davis, L., Breyer, R. M. and Breyer, M. D. (2000) Characterization of murine vasopressor and vasodepressor prostaglandin E_2 receptors. Hypertension. 35(5), 1129–1134.
36 Thompson, E. J., Gupta, A., Vielhauer, G. A., Regan, J. W. and Bowden, G. T. (2001) The growth of malignant keratinocytes depends on signaling through the PGE_2 receptor EP1. Neoplasia. 3, 402–410
37 Heo, J. S., Lee, Y. J. and Han, H. J. (2006) EGF stimulates proliferation of mouse embryonic stem cells: involvement of Ca^{2+} influx and p44/42 MAPKs. Am. J. Physiol. Cell. Physiol. 290(1), 123–133.
38 Jin, Y., Wang, Z., Zhang, Y., Yang, B. and Wang, W. H. (2007) PGE_2 inhibits apical K channels in the CCD through activation of the MAPK pathway. Am. J. Physiol. Renal Physiol. 293(4), 1299–1307.
39 Heo, J. S., Lee, M. Y. and Han, H. J. (2007) Sonic hedgehog stimulates mouse embryonic stem cell proliferation by cooperation of Ca^{2+}/protein kinase C and epidermal growth factor receptor as well as Gli1 activation. Stem Cells. 25(12), 3069–3080.
40 Slomiany, B. L. and Slomiany, A. (2004) Src-kinase-dependent epidermal growth factor receptor transactivation in salivary mucin secretion in response to β-adrenergic G-protein-coupled receptor activation. Inflammopharmacology. 12(3), 233–245.
41 Zhang, H., Chalothorn, D., Jackson, L. F., Lee, D. C. and Faber, J. E. (2004) Transactivation of epidermal growth factor receptor mediates catecholamine-induced growth of vascular smooth muscle. Circ. Res. 95, 989–997.
42 Gutkind, J. S. (2000) Regulation of mitogen-activated protein kinase signaling networks by G protein-coupled receptors. Sci. STKE. 40, 1–13.
43 Kim, Y. H., Heo, J. S. and Han, H. J. (2006) High glucose increase cell cycle regulatory proteins level of mouse embryonic stem cells via PI3-K/Akt and MAPKs signal pathways. J. Cell. Physiol. 209(1), 94–102.
44 Tian, Y., Sommerville, L. J., Cuneo, A., Kelemen, S. E. and Autieri, M. V. (2008) Expression and suppressive effects of interleukin-19 on vascular smooth muscle cell pathophysiology and development of intimal hyperplasia. Am. J. Pathol. 173(3), 901–909.
45 Miyahara, T., Katoh, T., Watanabe, M., Mikami, Y., Uchida, S., Hosoe, M., Sakuma, T., Nemoto, N., Takayama, K. and Komurasaki, T. (2004) Involvement of mitogen-activated protein kinases and protein kinase C in cadmium-induced prostaglandin E_2 production in primary mouse osteoblastic cells. Toxicology. 200(2–3), 159–167.
46 Manole, D., Schildknecht, B., Gosnell, B., Adams, E. and Derwahl, M. (2001) Estrogen promotes growth of human thyroid tumor cells by different molecular mechanisms. J. Clin. Endocrinol. Metab. 86, 1072–1077.